

Heat-induced changes in soil properties: fires as cause for remobilization of chemical elements

Hana Fajković¹, Maja Ivanić^{2*}, Ivan Nemet³, Sanda Rončević³, Štefica Kampać¹, Dana Leontić Vazdar¹

¹ Department of Geology, Faculty of Science, University of Zagreb, Horvatovac 102a, 10 000 Zagreb, Croatia.

² Division for Marine and Environmental Research, Ruder Bošković Institute, Bijenička c. 54, 10 000 Zagreb, Croatia.

³ Department of Chemistry, Faculty of Science, University of Zagreb, Horvatovac 102a, 10 000 Zagreb, Croatia.

* Corresponding author. Tel.: +385 1 456 1176. E-mail: mivanic@irb.hr

Abstract: Exposure of soil constituents to elevated temperatures during wildfire can significantly affect their properties and consequently, increase the mobility of the bound contaminants. To estimate the potential of wildfires to influence metal remobilization from the burned soil due to the changes in cation exchange capacity (CEC) after organic matter combustion and mineral alteration and degradation, changes in soil properties after exposure to different temperatures was investigated. This was accomplished through analysis of geochemical, mineralogical and surface physicochemical properties of a soil sample exposed to different temperatures in a laboratory. Heating the soil sample at 200 °C, 500 °C and 850 °C resulted in an increase in pH (from 5.9 to 12.3), decrease in cation exchange capacity (from 47.2 to 7.3 cmol·kg⁻¹) and changes in the specific surface area (observed only at 500 °C), that are associated with structural modifications of clay minerals and ferromagnetic minerals. Extraction analysis showed the increase in the concentration of almost all analysed elements (Al, Cd, Co, Cr, Fe, Mn and Zn) in soil eluates. The observed increase, following high-temperature heating (500 °C and 850 °C), was as much as 15 times higher (e.g., Al), compared to the native soil sample (25 °C). This strongly indicates that wildfire can act as a trigger for remobilization of heavy metals.

Keywords: Heating; Soil; Trace metals; Physicochemical properties.

INTRODUCTION

Over 48,000 forest fires are recorded in Europe annually and most of them occur in the Mediterranean region (Dupuy et al., 2020; Moreno, 2014), especially during summer months. The year 2019 was the worst-ever year for forest fires around the world in recent history with burned area of natural land in Europe over 400,000 ha (Commission report, 2020), and the years that followed were not much better. By Joint Research Centre (JRC) in the 2021 was recorded 1 113 464 ha burned area (San-Miguel-Ayanz et al., 2022). According to some wildfire regime concepts defined by pattern, frequency, and intensity of the wildfires over long periods of time it is predicted that fire activity will increase to the end of the century (Duane et al., 2019), while Moriondo et al. (2006) are expecting that the intensity of wildfires, duration of the fire seasons, the number of days in each season facing extreme fire risk, as well as the areas burned by wildfires per year will increase in the future.

Fire, whether prescribed or wildfire, affects many different properties of soil, as described by many authors (Alcañiz et al., 2018; Fernandez-Marcos, 2022; Francos et al., 2018; Santin and Doerr, 2016). It is also important to emphasise that contaminants, i.e., potentially toxic elements, are often constituents of a soil that can become immobile over time, although the possibility of redistribution exists. Such immobilisation can occur as a result of the ion binding capacity of the soil, i.e., the cation exchange capacity (CEC). The presence of clay minerals and OM in soils increases the CEC and consequently the mobility of potentially toxic elements tends to be lower (Palansooriya et al., 2020). Changes or degradation of the mentioned soil components are of extreme

importance when thinking about remobilisation, and such remobilisation can occur when the soil is exposed to fire.

A review paper by Santin and Doerr (2016) defines three main directions of influence of fire: Influence of heating and combustion processes (i); indirect influence through changes in vegetation cover (ii); and redistribution of soil through post-fire erosion. A review of the research regarding the effects of the prescribed fires on the physical, chemical, and biological soil properties by Alcañiz et al. (2018) emphasized that the physical and biological properties are more significantly affected than the chemical ones, particularly for low intensity fires. Francos et al. (2018) showed that high-intensity fires also alter the soil chemical properties. Mineral particles and soil organic matter (SOM) control the cation exchange capacity and the available surface area of soil (Deng and Dixon, 2002; Schulze, 2002). Mineralization of organic matter, as a consequence of wildfires, was already associated with elevated concentrations of metals in water bodies (Abraham et al., 2017; Ignatavičius et al., 2006) and is considered as the main source of metals in the post-fire environment. Phyllosilicates, an omnipresent group of minerals in soils and sediments, due to their generally small particle size, large surface areas and affinities for exchange of cations with the surroundings, exhibit a strong influence on the soil properties.

Changes of these constituents can affect the mobility of metals stored in soil, which can, in consequence, combined with the post-fire rain runoff and wind erosion, seriously affect the water resources associated with the burned area (Abraham et al., 2017; Campos et al., 2016 and references therein). Roughly, at temperatures close to 100 °C most living organisms and nutrient cycling processes are affected, when the temperature reaches 400 °C organic matter is destroyed, while

at even higher temperatures (>450 °C) the structure and properties of mineral particles, especially clay minerals, begin to alter (Neary et al., 2005). It was shown that in soils with increased content of clay minerals and organic matter, the mobility of metals is low (Abraham et al., 2017; Yoon et al., 2006), suggesting that alterations of these soil constituents, as in the case of wildfires, has an inevitable impact on the soil properties (Reynard-Callanan et al., 2010) and could increase the mobility of heavy metals. The important contribution of wildfires on the levels of major and trace elements in the burned soil and ash and their potential mobilization were already suggested (Campos et al., 2016; Costa et al., 2014; Ignatavičius et al., 2006; Odigie et al., 2016; Pereira and Úbeda, 2010). In a recent review on post-fire metal concentrations in soil, Abraham et al. (2017) highlight the lack of information regarding behaviour of metals in soils affected by wildfires, especially considering Co, Cu, Cr, Cd, Ni, Zn and As. The temperatures achieved during the fire and duration of the fire itself are two of the main parameters influencing the extent to which the soil properties are affected (Certini, 2005; Santin and Doerr, 2016). Along with field investigations on the fire affected areas (Ulery et al., 2017) laboratory studies are often applied in investigation of fire-induced changes in soil properties (Araya et al., 2016; Marcos et al., 2007; Pape et al., 2015). When observing soil changes caused by fires, one finds that some changes occur shortly after the fire event, while others occur in the long term, as described in a review by Fernandez-Marcos (2022). From the point of view of this research, the research interest lies in short-term changes that occur after the fire and could be the result of the redistribution of potential toxic elements previously immobilised by organic matter and some minerals.

A laboratory investigation of the effect that different temperatures have on soil properties allows an assessment of alterations that low-, medium- and high-intensity fires, could exhibit on the mineral composition of a soil sample and its surface physicochemical properties. Analysis of major and trace metals released from the soil sample at different heating temperatures, allows assessment of the potential mobility of major and trace metals at different heating temperatures and its linkage with the determined alterations of soil constituents. This study aims to broaden the knowledge on the effect of heating on the surface physicochemical (the specific surface area and the cation exchange capacity), geochemical and mineralogical properties of a soil sample, and evaluate the influence this exhibits on the release of the associated trace metals. By comparing the amount of leachable chemical elements from soil heated at different temperatures, in parallel with a detailed geochemical and mineralogical analysis of the heated soil, it will be possible to better understand and separate the influence of fire on the remobilisation of formerly immobilised elements due to degradation and/or changes in mineral structure and organic matter.

In general, it contributes knowledge on the potential severity of wildfires impact on the surrounding environment through release of potential contaminants. The sampled soil represents a typical Croatian forest soil, that is most frequently affected by wildfires and as such provides information important for environmental protection on a regional scale due to better understanding of system. Since the pollution of water and the aquifers has already been associated with the fires (Burke et al., 2013; Úbeda and Sarricolea, 2016), the emphasis on such scenarios is of crucial importance in the karstic areas, prevailing in the Croatian coastal area, due to the aquifer position and the possible high rate of pollutants transfer.

MATERIALS AND METHODS

Study area, sampling and sample preparation

As in the other Mediterranean countries, the summer months in Croatia are characterized by long, dry periods with high temperatures and droughts. The coastal areas are under additional fire risk due to frequent winds that easily change speed and direction and the terrain that is mostly covered with easily flammable vegetation (dry grass, bushes and Mediterranean shrubland-maquis) or coniferous forests of Aleppo pine (*Pinus halepensis* Mill.) and Evergreen oak (*Quercus ilex* L.) (Pavlek et al., 2016). Furthermore, the concentration of a large number of people in the coastal areas due to touristic activities increases the possibility of fire occurrence. According to the EFFIS (European Forest Fire Information System) annual fire reports, 113 forest fires were registered by satellite imagery in Croatia in the year 2021, with 3 779 ha of burned forest area (out of the total burned area of 10 074 ha), mostly in southern Dalmatia, the region most frequently exposed to fires (Šiljković and Mamut, 2016).

A typical forest soil from northern Dalmatia (Croatia), characterized by a mild Mediterranean climate and a dominant vegetation of Aleppo pine (*Pinus halepensis* Mill) (Tekić et al., 2014), was sampled (location coordinates: N43°55'43.62" and E15°29'27.83"), defined as Csa climate type according to the Köppen-Geiger climate classification (Nimac and Tadić, 2016). The Aleppo pine is among the most important species in the Mediterranean, covering an area of more than 25,000 km² (Šiljković and Mamut, 2016). The sampled soil was classified as *terra rossa*, shallow and medium deep (Bogunovic et al., 2011), not affected by wildfires in the recent years before sampling. Since the downward heat transfer during the fire is not as effective, especially in dry soils (Neary et al., 2005), only the surficial soil layer (0–2.5 cm) was collected with a plastic trowel, afterwards air-dried at room temperature and homogenized.

Soil heating

Heating of the soil in a muffle furnace is a well-known laboratory technique used to imitate the direct impact of a wildfire in a sense to observe changes that different temperatures and the exposure time, the so-called contact time, could induce on the soil sample (Albalasmeh et al., 2013; García-Corona et al., 2004; Soto et al., 1991; Thomas and Fachin, 2014). Various contact times can be found in the literature, from 20 minutes to 18 h, while the heating temperatures range from 20 °C to 1093 °C. For the purposes of this study, a homogenized soil sample from the location described in previous section was divided into four sub-samples, and each sub-sample was investigated in parallel. The prepared sub-samples were heated for 2 h at 200 °C, 500 °C and 850 °C. Defined heated temperatures should indicate and include changes related with the CEC: structural changes of some Fe (oxy)hydroxides that occurs in a lower temperature range starting from 200 °C (i); organic matter decomposition that at 500 °C should be removed (ii); alteration and changes in structure of some clay minerals and Fe (oxy)hydroxides that should be finished at 850 °C (iii). The native soil sample is henceforth referred to as treated at 25 °C. The selected contact time, e.g., 2 h, is in accordance with the investigations of Gray and Dighton (2009) and Úbeda et al. (2009) and based on the possibility that some changes could be undetected in a shorter time period, like in several other methodologies (Arce-negui et al., 2007; Mataix-Solera et al., 2014). The heating temperatures were also selected in accordance with the observed changes and the results of previously mentioned studies.

Granulometric and physicochemical (SSA, CEC, pH, C_{org}, CaCO₃) characteristics of soil

The granulometric characterization was performed on soil sub-samples using the laser diffraction on LS 13320 (Beckman Coulter, USA). The particle size was determined according to the modified Wentworth (1922) grade scale with the clay-silt boundary at 2 µm. Prior to measurements, the soil samples were soaked in deionized water overnight and treated with an ultrasound for 5 min. All measurements were performed in triplicates.

The soil pH was determined using a glass electrode pH meter according to the standard methods (Kalra, 1995). The specific surface area (SSA) triplicates were determined by a single-point nitrogen adsorption using the BET method, on a Flow-Sorb II 2 300 instrument (Micromeritics, USA). The cation exchange capacity (CEC) measurements were performed using the ammonia selective electrode, according to the method described by Busenberg and Clemency (1973). All measurements were performed in duplicates.

The soil organic carbon (C_{org}) determination and the carbonate content (CaCO₃) was performed only on untreated (25 °C) homogenized subsamples, due to the organic matter combustion and carbonates decomposition at the higher temperature. Soil organic carbon (C_{org}) was determined by the loss-on-ignition procedure according to Wang et al. (2012) on 1 g of homogenized soil, in triplicates. The carbonate content analyses were performed on homogenized subsamples according to the EN ISO 10693 (2014) using Scheibler calcimeter. The mass of the analysed samples was ~500 mg, and analyses were performed in triplicates.

Mineralogical analysis of soil samples

The mineral composition was determined using a Philips X'pert powder diffractometer with CuK α radiation from the tube operating at 40 kV and 45 mA, with the X-ray diffraction data set collected from 4° to 63° 2 θ . The mineralogical analysis was performed on the bulk soil sub-sample, on the clay fraction and on the ferromagnetic fraction, after each heating. A detailed analysis of clay minerals was performed according to Moore and Reynolds (1997). After the separation, the clay fraction (<2 µm) was air-dried, treated with ethylene glycol, and heated at 400 °C and 550 °C for 30 minutes. For the analysis of the ferromagnetic fraction the ferromagnetic minerals were separated from a water suspension of an equal amount of the bulk sub-sample using a magnet, from each sample after heating.

Fourier transform infrared (FTIR) spectra were carried out on a Bruker Tensor 27 in the region from 400–4000 cm⁻¹, on the clay fraction (<2 µm) separated from the heated samples and on the separated ferromagnetic minerals. The measurements were performed on the KBr pellets, prepared by the hydraulic press.

Geochemical analysis of soil samples

The geochemical analyses were carried out with the goal to determine if different contact time will influence the concentration of the mobile fraction of chemical elements. The mobile fraction of elements was obtained from the first step of the modified BCR sequential analysis (Rauret et al., 1999). The first step of the BCR procedure uses 0.11 mol L⁻¹ CH₃COOH to extract the exchangeable phase and phase bound to carbonates. Production of the extracts was performed on 1 g of soil, and the extracts separation was achieved by centrifuging at 3000 rpm for 30 min and the supernatant was filtered through membranes with the 0.45 µm pore size. The concentrations of the selected

chemical elements (Al, Cd, Co, Cr, Cu, Mn, Fe, Zn) in the extracts were determined by the inductively coupled plasma optical emission spectroscopy (ICP-OES) using Teledyne Leman Labs (Hudson, NH, USA) Prodigy High Dispersion ICP. The geochemical analyses were performed on all sub-samples (25 °C – 850 °C), in duplicates.

RESULTS

Granulometric and physicochemical (SSA, CEC, pH, C_{org}, CaCO₃) characteristics of soil

The investigated untreated soil sample (25 °C) contained mostly silt (46%) and sand (40%) sized particles with 14% of clay fraction. Two distinct trends can be observed from the exposure of the soil sample to high temperatures (Fig. 1a): (i) lowering of the particle mean size (Mz) at 200 °C and 500 °C, due to an increase in silt fraction and a decrease in the sand content (minor increase in the share of clayey particles occurred at 200 °C), and (ii) coarsening of the soil texture at 850 °C due to an increase in the sand fraction and a decrease in the content of silt-sized and clayey particles. It can be observed from the particle size distribution (PSD) curves, that at temperatures above 500 °C, the modes observed in the untreated sample (25 °C) and the sample heated at 200 °C disappear, and unimodal curves prevail. All samples were classified as sandy silt (Shepard, 1954) as presented in a ternary diagram (Fig. 1b).

The heat-induced changes in pH, CEC and SSA are shown in Figure 2. Duplicate measurements were performed, and results were reported as the mean values with the standard deviation (\pm). An increase in the soil pH, from slightly acid (5.9 \pm 0.2) at 25 °C to alkaline (12.3 \pm 0.1) at 850 °C was observed with heating. While the initial heating (200 °C) exhibited no effect on the pH, at 500 °C the pH increased to 7.3 \pm 0.2 and the highest pH (12.3 \pm 0.1) was determined in the sample heated at 850 °C. Similarly, the CEC values remained unchanged after the initial heating at 200 °C (from 47.2 \pm 4.24 cmol \cdot kg⁻¹ at 25 °C to 46.9 \pm 3.02 cmol \cdot kg⁻¹ at 200 °C). However, further heating caused lowering of CEC to 26 \pm 1.69 cmol \cdot kg⁻¹ at 500 °C, and even lower value was determined in the sample heated at 850 °C, 7.3 cmol \cdot kg⁻¹. The results showed similar SSA values in the samples treated at 25 °C, 200 °C and 850 °C (18.7 \pm 0.43 m² g⁻¹, 20.9 \pm 0.48 m² g⁻¹ and 18.5 \pm 0.53 m² g⁻¹, respectively), while over 3 times higher value, 71 \pm 1.17 m² g⁻¹, was obtained for the sample heated at 500 °C.

C_{org} and CaCO₃ were measured only on an untreated soil sample (25 °C). Triplicate experiments were performed, and results were reported as the mean values with the standard deviation (\pm). The measured values were 139.94 \pm 5.6 g kg⁻¹ and 4.54 \pm 0.1 % for C_{org} and CaCO₃, respectively.

XRD and FTIR analysis

XRD analysis of all bulk soil sub-samples produces similar diffraction patterns, with the quartz (2 θ at 26.63°, 20.84° and 50.12°) established as the prevailing mineral phase (Fig. S1), and some additional peaks (2 θ at 19.97°, 28.05° and 35.07°), probably from the mica and clay group of minerals. Due to the low share of the mica group in bulk sub-samples some uncertainties in determination are present. The XRD analysis of the clay fraction (<2 µm) presents similar diffraction patterns for all analysed sub-samples but with the several differences among analysed samples. It refers as an increase in peak intensity and appearance of additional peaks at temperatures above 200 °C associated with the clay minerals from the kaolinite group, mainly halloysite (2 θ at 19.98, 26.58 and 29.45) (Fig. S1).

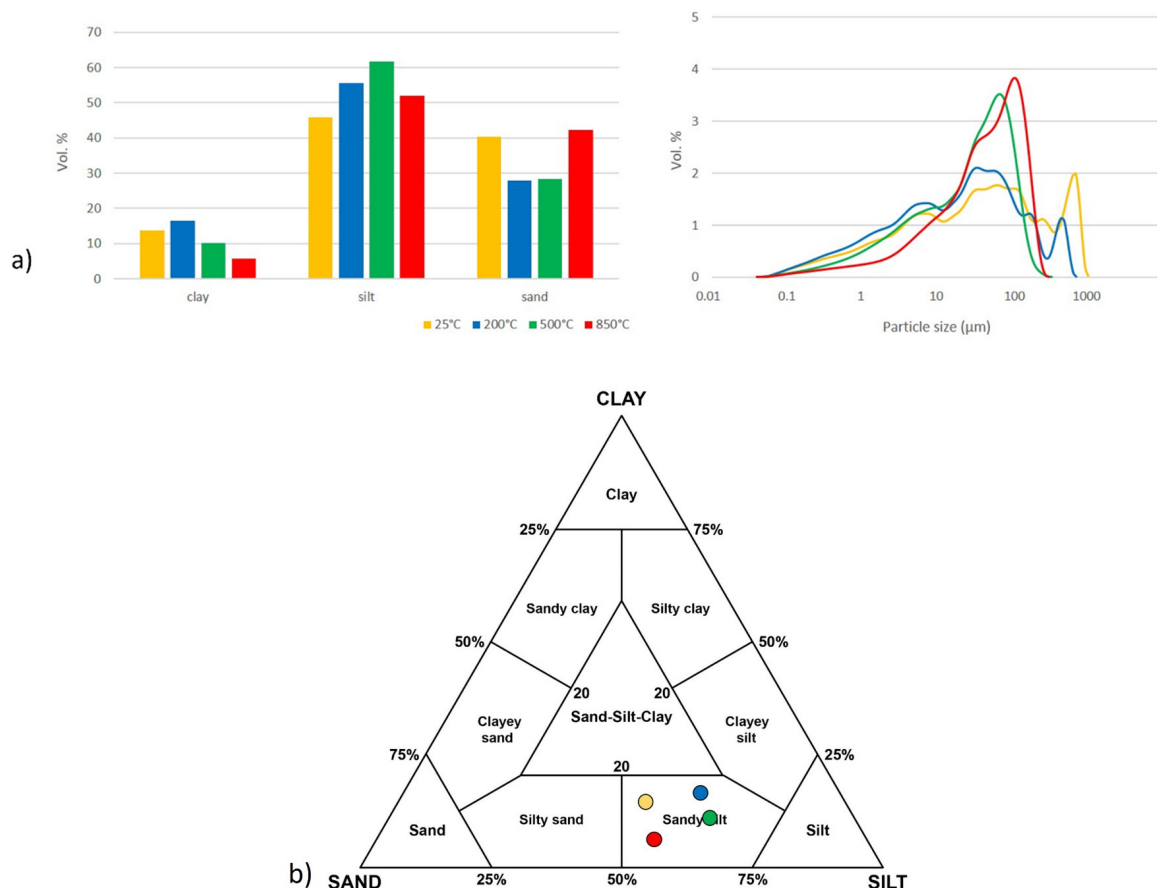


Fig. 1. Changes in the share of clay, silt and sand fraction (left) and the particle size distribution (PSD) curves (right) of the investigated samples heated at different temperatures (a) and ternary diagram for classification of sediments (Shepard, 1954) (b).

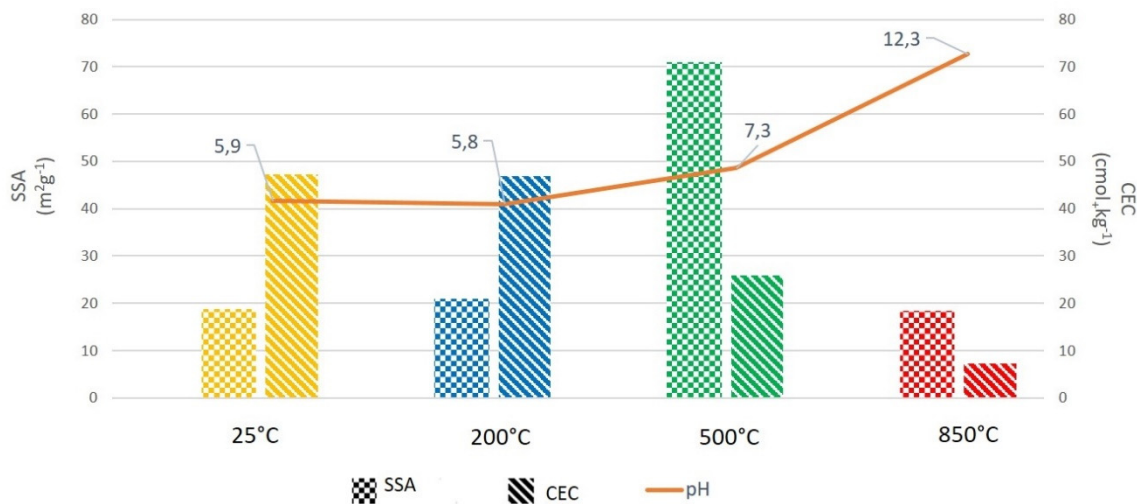


Fig. 2. The heat-induced changes in the specific surface area (SSA), the cation exchange capacity (CEC) and the pH of the investigated soil sample.

The ferromagnetic minerals for XRD and FTIR analysis were isolated from the same amount of the bulk sample. It was observed that the amount of ferromagnetic minerals varied in samples heated at different temperatures: their content was low in the unheated sample (25 °C), slight higher in the sample heated at 200 °C, significantly increased at 500 °C, while at 850 °C they were hardly present in the sample (Fig. S2). The diffraction patterns of the ferromagnetic minerals collected from the unheated sample, at 25 °C, showed magnetite and/or ma-

ghemite as the main Fe-bearing mineral phase (Fig. S1). Heating caused appearance of additional peaks on the diffraction patterns, as well as changes in the peak intensity. The peak (2θ) at 31.68° is present only at 25 °C and 850 °C. The peak (2θ) at 33.25° at 850 °C indicates the transformation of magnetite/maghemite minerals to hematite.

FTIR spectra of the analysed clay fraction (<2 μm) and ferromagnetic minerals, shown in Figure 3, are recorded in the region 400–4000 cm⁻¹. The spectra of the clay fraction

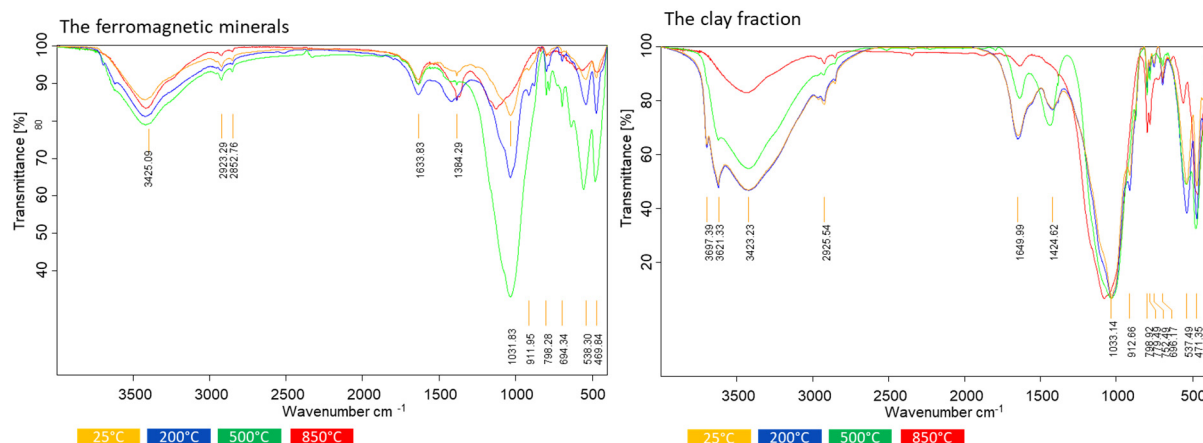


Fig. 3. Results of the FTIR analysis of the ferromagnetic minerals (left) and the clay fraction (right) isolated from the bulk soil samples treated at different temperatures.

Table 1. The weight fraction of analysed elements by first step of BCR sequential analysis (mean \pm standard deviation).

	Al	Ba	Cd	Co	Cr	Cu	Mn	Fe	Zn
	w (mg kg ⁻¹)								
25 °C	59.39 \pm 5.28	37.11 \pm 1.67	0.45 \pm 0.018	1.14 \pm 0.05	LoD *	1.06 \pm 0.06	283.58 \pm 9.93	7.61 \pm 0.41	LoD
200 °C	108.50 \pm 7.70	33.93 \pm 1.32	0.59 \pm 0.027	3.57 \pm 0.14	0.29 \pm 0.02	LoD	491.81 \pm 23.60	11.19 \pm 0.40	5.43 \pm 0.65
500 °C	894.82 \pm 56.36	30.38 \pm 1.46	0.49 \pm 0.03	3.70 \pm 0.17	0.72 \pm 0.04	LoD	458.04 \pm 21.53	117.78 \pm 3.65	26.29 \pm 1.7
850 °C	666.84 \pm 45.01	13.92 \pm 1.36	0.20 \pm 0.016	0.49 \pm 0.02	16.26 \pm 0.49	1.82 \pm 0.13	26.65 \pm 1.31	21.10 \pm 1.01	--- **

* LoD Under limit of detection, --- lost of sample

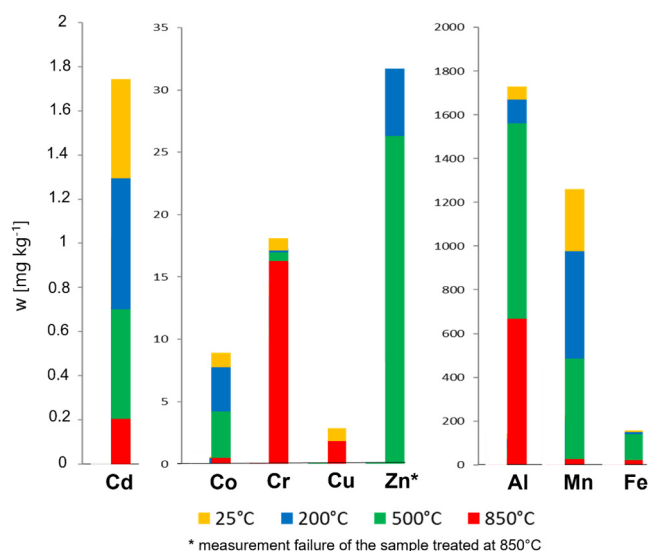


Fig. 4. Distributions of the analysed elements in soil heated at different temperatures, determined by the first step of the BCR extraction procedures.

(< 2 μ m) from the untreated sample (25 °C) and the sample heated at 200 °C were similar, overlapping in most of the spectrum. Disappearance of the absorption bands in the samples heated at 500 °C (3697 cm⁻¹ and 3621 cm⁻¹) and 850 °C (1420 cm⁻¹) were observed. Vibrational bands match the one for halloysite. The FTIR analysis of the ferromagnetic minerals showed similar pattern of the absorption bands in the region

3500–1500 cm⁻¹, while changes were observed in the region from 1500–400 cm⁻¹ (Fig. 3). Similar absorption bands in all samples were observed at 3425 cm⁻¹, 2923 cm⁻¹, 2853 cm⁻¹ and 1634 cm⁻¹. A shift of several bands (1384 cm⁻¹ and 1031 cm⁻¹) was observed in samples heated at different temperatures, while several bands changed intensity (538 cm⁻¹ and 469 cm⁻¹). In the sample heated at 500 °C new vibration bands were detected (at 874 cm⁻¹, 713 cm⁻¹, 539 cm⁻¹ and 477 cm⁻¹).

Changes in concentrations of major and trace elements with heating

The results of the geochemical analysis are presented in Table 1 and Figure 4. Similar changes in concentrations with heating were observed for Al, Co and Fe, their concentrations in extracts increased up to 500 °C, where the maximum concentrations in extracts were attained. The most significant changes in concentrations were observed at 500 °C for Al and Fe, and at 200 °C for Co. Lower concentrations of these metals were attained in extracts after heating at 850 °C, even though in the case of Al and Fe the released concentrations were still higher than at 200 °C, while for Co the extracted concentration was lower than in the unheated sample. Similar was observed for Mn and Cd, but the maximum concentration in the extracts was attained at 200 °C. The concentrations in the extracts at 500 °C did not change significantly, while at 850 °C they decreased to values even lower than in the unheated sample. While the concentration of Cu in the extract generally lowered with heating, a slight increase occurred at 850 °C. The extracted concentrations of Cr increased continuously with heating, reaching a maximum, and the highest increase, at 850 °C. Similar was observed for Zn, even though the measurement at 850 °C is missing.

DISCUSSION

In order to assess the possible effects of wildfires on the soil geochemistry, hydrogeology and physicochemical properties, a sample of a representative forest soil was heated at different temperatures in the laboratory, with contact time set on 2 h. The results showed important changes in soil properties and geochemistry occurring at specific temperatures that can be related to transformations of mineral phases in the soil.

Quartz, the most abundant mineral in the analysed soil samples, changes its structure with heating into different SiO₂ polymorphs. According to Hajpál and Török (2004), in the explored temperature range, from 25 °C – 850 °C, quartz should transform from α -quartz to β -quartz at 580 °C – 595 °C, and transformation is also associated with the volume increase, whereas tridymite is formed at 873 °C. Described volume transformation could contribute to observed change in the granulometric composition (Fig. 1.) with the temperature, also described by some authors (Aasly et al., 2007; Zobnin et al., 2018). The transformation from α to β -quartz is fast and reversed during cooling (Ringdalen, 2015).

Halloysite and kaolinite are more thermally instable compared to quartz. Their thermal reactions can be divided into four steps, namely a low-temperature reaction at < 400 °C, intermediate-temperature reactions, mainly between 400–650 °C, high-temperature reactions at > 700 °C and oxidation reactions (Liu et al., 2015). By Liu et al. (2015) kaolinite will be transformed to metakaolin at heating up to 600 °C and the peak temperature of the dehydroxylation is at ~ 600 °C. The metakaolin transformed into γ -alumina, or aluminium-silicon spinel and amorphous silica after decomposition at 900 °C, followed by mullite at 1200 °C and α -cristobalite at 1400 °C. The mentioned temperatures should be taken with caution for each specific sample since the transformation is influenced by the type and the amount of impurities and phase disorder of the minerals. During the heating process the surface area (SSA) increases by 10 %, in the temperature range from 500 °C to 850 °C, after which it starts to drop to the value lower than that of the untreated sample (Sennett, 1990). In analysed samples the value of SSA first increased at the temperatures of 200 °C and 500 °C, and afterwards SSA decrease for the temperature of 850 °C. As described, the particle aggregation and transformation to metakaolin will occur with the temperature rise, from 500 °C up to 1000 °C. This can also influence the results of the granulometric analysis and the observed sand increase at 850 °C. The reaction mechanism under heating of halloysite has been postulated to be analogous to that of kaolinite due to their chemical and structural similarities (Yuan et al. 2012). According to the same author some differences occur, such as dihydroxylation at the lower temperatures from ~500 °C to ~900 °C. Maghemite is a ferromagnetic mineral with the same chemical composition as hematite but with the structure similar to magnetite, and due to their similar crystal structure, maghemite and magnetite have the similar magnetic property (Liu et al., 2010). The reported transition temperatures of maghemite vary widely, from 250 °C to 900 °C and it is usually described as thermally unstable, with conversion to hematite above 250 °C (Liu et al., 2010), accompanied by a surface area reduction (Sidhu, 1988). Type of magnetism is also significantly different among Fe oxides, maghemite and magnetite on the one hand, and hematite on the other. The first minerals are ferrimagnetic, while hematite is weakly ferromagnetic or antiferromagnetic (Mammucari, 2008). In analysed samples transformation from magnetite/maghemite to hematite is observed (Fig. S1) together with the decrease of the amount of ferromagnetic particles (Fig. S2)

which is associated with the changes in magnetism. Changes of SSA, more accurately major increase of SSA value at 850 °C, can also be explained by observed mineral transformation. According to the results high-temperature burns (500 °C and 850 °C) induced changes in the soil texture and structure, that can be related to organic matter removal, dehydration of clays and mineral transformation (Fig. 1). Coarsening of the soil particles, e.g. increase in the sand fraction, as observed at 850 °C, was found to occur in studies involving temperatures above 600 °C (Ketterings et al., 2000) and even lower temperature ranges (Pape et al., 2015). Removal of SOM, a cementing agent in organo-mineral aggregates, strongly affected their stability. According to García-Corona et al. (2004), the loss of SOM can be already noticed at 220 °C, 55–63% of carbon is lost at 380 °C, and the complete removal of SOM occurs at 500 °C. Indeed, a change in granulometric characteristics, e.g., increase in silty fraction on account of clayey particles, was observed after heating at 500 °C, that can be related to the SOM removal. This was even more intensified after heating at 850 °C, where clayey and silty fraction is reduced on account of sand. At this temperature all SOM is removed, and particles can re-aggregate and formation of strong mineral aggregates occurs, causing the observed redistribution of particle size in the high-temperature sample. Heat induced recrystallization of aluminosilicates and metal oxides can also cause strong aggregation of clayey particles and induce higher share of coarse particles (Mataix-Solera et al., 2014). The observed increase in pH (Fig. 2) was already associated with soil heating (Certini, 2005; Kettering et al., 2000; Pape et al., 2015) and related to the SOM destruction, formation of oxides, hydroxides and carbonates. The initially similar values in the unheated sample and sample heated at 200 °C are in agreement with other obtained results, suggesting little or no change in the sample composition and properties at this temperature. This is in accordance with Pereira et al. (2019), suggesting that the increase in pH is not expected to occur at temperatures lower than 300 °C. Increase in pH values at 500 °C can be related to the mineralization of SOM, and the associated release of basic cations (Neary et al., 2005), and the formation of oxide, hydroxide and carbonates. The most significant increase in pH, observed at 850 °C, can be related to the ash formation and the additional increase in the cation content, during which alkalinity can be achieved (Neary et al., 2005). CEC is a soil property that defines the capacity of a soil to store charged ions. The soil CEC is associated with the SOM and clay minerals, while heating affects both components (Ulery et al., 2017). The temperatures at which changes in soil properties begin to occur are expected in the range of 250 °C and 450 °C, depending on the initial changes in the SOM, since mineral alterations occur at higher temperatures. However, different temperatures are reported in the literature. For example, Pape et al. (2015) found significant loss of CEC and SOM from topsoil already at temperature of 250 °C, while Inbar et al. (2014) reported decrease of CEC at temperature of 300 °C and assigned it to loss of SOM and dehydration of clay minerals 2:1, while Soto and Diaz-Fierros (1993) found most significant loss of CEC at 380 °C.

In this study, the initial heating (at 200 °C) exhibited no effect on the investigated soil properties (Fig. 2). A significant lowering of CEC observed at 500 °C, by 45%, is in accordance with the finding of Araya et al., (2016) who found statistically significant changes in CEC after heating at 450 °C. This can be related mostly to the SOM destruction and partially to the dehydration of clay minerals, seen as a disappearance of bands in a high-frequency region (4000 – 3000 cm⁻¹) and decomposition of kaolinite which, according to Ulery et al. (2017) occurs

from 420 °C to 550 °C, and results in appearance of amorphous aluminosilicates. These particles, in addition, can be responsible for the aggregation of mineral particles (Ulery et al., 2017) which is supported by the changes in PSD curves and the observed coarsening of the grain size occurring between 500 °C and 850 °C (Fig. 2). The final and the most notable decrease in CEC, by 73%, observed at 850 °C (Fig. 2), can be related to the collapse of structure of clay minerals, and their subsequent inability to retain cations (Fig S2). Similar was observed by Soto and Diaz-Fierros (1993), where the change in CEC after heating at 170 °C was insignificant, most significant loss in CEC occurred after heating at 380 °C and after heating at 700 °C complete loss of CEC occurred. It seems that most of the CEC loss was related to collapse of mineral structure, which has longer effect on the topsoil surface properties (Ulery et al., 2017). The CEC of iron oxides is low (Ulery et al., 2017) and its contribution is not significant in soil CEC. The CEC of kaolinite is not high, but halloysite can have higher CEC (Ivanić et al., 2015; Kabata-Pendias, 2010). The results show that heating of soil modifies its capacity to exchange cations.

The effect of heating on the SSA, a property of solids defined as the total surface area per unit of mass, was only visible in the sample treated at 500 °C, where over 3 times higher SSA values were obtained (Fig. 2). This increase is even more conspicuous given the fact that the SSA decreased to its initial values after heating at 850 °C (Fig. 2). A possible explanation could be found in the content of ferromagnetic minerals, which was highest at 500 °C, after which, at temperature of 850 °C, their share was negligible (Fig. S2). The observed could be related to the appearance of secondary magnetic minerals, mostly hematite. Magnetic susceptibility of maghemite is much higher than that of hematite, and it is a temperature-dependent on value with the Curie temperature around 635 °C (Gehring et al., 2009; Liu et al., 2010). The transformation to ferromagnetic minerals with higher magnetic susceptibility starts to occur at lower temperatures, but is most notable at temperatures above 500 °C (Gedye et al., 2000). According to Guo and Barnard (2013), hematite nanoparticles formed during wildfires can have smaller sizes compared to the low-temperature formed hematite, which could also contribute to the increased SSA observed at 500 °C. Araya et al. (2016) found that the heat-induced changes in SSA below 500 °C are related to physical disintegration and charring of SOM, and not soil mineralogy. This may be the case in some soil samples, and the fact that Araya et al. (2016) had more heating steps in the temperature range up to 450 °C, however we found no changes in SSA and the only change at 500 °C can be related to the changes in mineralogy. The results of the more detailed XRD investigation (Fig. S1) on the ferromagnetic fraction suggest the presence of hematite or aggregates of maghemite and hematite (Bigham et al., 2002; Boski and Herbillon, 1988). More information was obtained from the FTIR absorption spectra of the separated ferromagnetic minerals (Fig. 3). According to Namduri and Nasrazadani (2008), maghemite has absorption bands at 630 cm^{-1} , 590 cm^{-1} and 430 cm^{-1} , with possible bands at 700 cm^{-1} , 630–660 cm^{-1} and 620 cm^{-1} , while those of hematite are positioned at 540 cm^{-1} , 470 cm^{-1} and 352 cm^{-1} . The absorption bands at 538 cm^{-1} and 469 cm^{-1} in samples 25 °C and 200 °C were assigned to hematite. The appearance of the same bands in the FTIR investigation of the ferromagnetic fraction, as in that of the clay fraction (Fig. 3), suggests their common occurrence in the soil in form of micro-aggregates. The new vibration bands (874 cm^{-1} , 713 cm^{-1} , 539 cm^{-1} and 477 cm^{-1}) appearing at 500 °C indicate occurrence of new phases that are no longer present at the temperature of 850 °C. These results are in good

accordance with the observed changes in SSA (Fig. 2). The absorption band at 700 cm^{-1} in samples treated at 500 °C and 850 °C and 647 cm^{-1} at 850 °C were assigned to maghemite. Since hematite is thermally inert, some changes can be associated with the water evaporation at 500 °C, making the absorption band clearer (Vassiliadou et al., 2009). A detailed XRD analysis of the clay fraction (<2 μm) showed changes in the mineralogical composition that occurred with heating (Fig. S1). The disappearance of the peak (2 θ) at 8.84° (10 Å) at 850°C (small intensity at 25 °C–500 °C), could be attributed to the alteration of halloysite. Two of the most common polymorphs of halloysite have the basal distance around 10 Å (hydrated form) and 7 Å, i.e. (2 θ) at 12.64° (dehydrated form). When heated above 60°C, dehydration of halloysite occurs, shifting the peak from 10 Å to 7 Å (Li et al., 2017). New peaks observed in the sample heated at 850 °C, positioned (2 θ) at 29.38°, 33.23° and 39.61°, and in the samples treated at 500 °C and 850 °C, (2 θ) at 29.38°, were attributed to the appearance of a new phase. The majority of the observed absorption bands of the infrared spectra obtained by FTIR (Fig. 3), were attributed to the halloysite/kaolinite mineral phase. The presence of kaolinite was indicated by the absence of a stronger band at 756 cm^{-1} than the one at 793 cm^{-1} . Additionally, these minerals rarely appear as pure phases, but rather as mixtures. Mixed phase of halloysite and kaolinite was determined due to the observed absorption peaks, and the fact that the absorption peak at 756 cm^{-1} was not stronger than the one at 793 cm^{-1} (Li et al., 2017).

From the results of the geochemical analyses by BCR procedure it can be concluded that the heating of soil induced release of major and trace metals. Aluminium is the most commonly observed substituent in pedogenic Fe oxides, due to their co-mobilisation during weathering and the abundance in nature. The extent of substitution of Al for Fe in hematite and maghemite ranges from 15 to 18 mole % (Bigham et al., 2002). Since the amount of Al in the analysed samples surpasses that of Fe (Table 1), it is more likely that it originates from the kaolinite group of minerals, namely kaolinite and halloysite, $\text{Al}_2\text{Si}_2\text{O}_5(\text{OH})_4$. Dehydroxylation of these minerals occurs from approximately 500 °C to 900 °C, leading to the loss of long-range order and increasing the disconnection of silica and alumina originally in the tetrahedral and octahedral sheets (Yuan et al., 2012). The observed finding is in accordance with the observed decrease of CEC (Fig. 2) and the increased concentration of Al extracted from the soil (Table 1). Namely, the concentration of Al increased for over 15 and 11 times in the samples treated at 500 °C and 850 °C, respectively, compared with the untreated sample (25 °C). Further, the complete organic matter decomposition occurs at 500 °C. At this temperature, the elements associated with OM are expected to be in a free form, which is probably observed as the increase in their concentrations at the temperatures of 500 °C and 850 °C (Fig. 4). A similar increase in concentration was observed for Co, Cr and Mn with elevated temperatures (Fig. 4). Even though the measurement for Zn in the sample treated at 850 °C is missing, the mentioned trend can be still observed at 500 °C. Extractability upgrowth was observed for all analysed elements, except Cu, from the untreated soil (25 °C) to the soil heated at 200°C, and even more for those heated at 500 °C and 850 °C. The maximum extractability growth was observed for Al. Due to a severe decrease in the content of ferromagnetic minerals in the sample treated at 850 °C, an increase of extracted Fe was expected to occur. Hence, the absence of higher concentration of Fe can relate to the transformation from maghemite to hematite. An important observation can be made from this analysis, con-

cerning the heating temperature. The concentrations of the chemical elements extracted in the first step of the mentioned procedures increased with the temperature rise. This suggests that heating, and consequently the specific temperature range developed in a wildfire, can have a more profound influence on the environment, especially on karst aquifers due to the specific path of possible contaminants. Furtheron, most of the models concerning the influence of pollutants on the environment are performed on the unheated sample as the untreated sample (25 °C), while the impact on the environment can be over 15 times higher, as shown for Al, when the sample is heated to 500 °C or 850 °C, as occurring during the fires.

CONCLUSION

The results of this laboratory work exhibit the effects of heating, simulating a wildfire, on the geochemical and physico-chemical characteristics of the soil. Following heating, the changes in concentrations of elements (Al, Cd, Co, Cr, Cu, Fe, Mn and Zn), pH, granulometric characteristics, specific surface area (SSA) and cation exchange capacity (CEC) were analysed and changes were observed. The changes in the mineralogical composition were assessed by means of a combined approach using the X-ray powder diffraction and the Fourier transform infrared (FTIR) spectroscopy. The main mineralogical changes were transformation of magnetite/maghemite minerals to hematite, and some structural changes of halloysite. The physico-chemical characterization of the soil samples showed similar behavior in the untreated (25 °C) and the low-temperature (200 °C) samples. Only at the temperatures above 200 °C notable changes in the investigated physicochemical parameters occurred. The increase in the temperature above 200 °C was followed by an increase in the pH values, and a decrease in CEC, both related to the organic matter destruction and the halloysite structure collapse. The samples heated at 500 °C and 850 °C, though granulometrically similar, showed different trends concerning the specific surface area, with a sharp increase in SSA observed at the 500 °C sample, followed by a decrease to the previous value at 850 °C. This was in accordance with the amount of the collected ferromagnetic minerals, reaching the maximum at 500 °C and the minimum at 850 °C. The observed structural changes within ferromagnetic minerals should be considered as a preliminary observation, but the observed is an indication suggesting that changes in iron oxide particles could be correlated with the observed SSA changes. A detailed analysis of the clay mineral fraction also suggested the structural changes occurring in the determined halloysite and kaolinite, with the temperature increase.

The geochemical analysis showed the increase in concentrations of Al, Cd, Co, Cr, Fe, Mn and Zn, in the exchangeable fraction, associated with the temperature rise. The maximum increase (15 times) was determined for Al, observed after heating the sample at 500 °C, compared to the untreated soil sample (25 °C). The increase in concentrations of all analysed elements, except Cu, with soil heating, strongly indicates that wildfire can act as a trigger for remobilization of the chemical elements.

This finding emphasizes the necessity of including the soil analysis in the wildfire-landscape relationship and the post-fire management, especially in the karstic areas with numerous fractures, where the soil cover can be as thin as a few cm, and where nothing is to prevent the migration of the mobilized elements, possible pollutants, into the aquifer.

Acknowledgements. This research was partially supported by the Croatian Academy of Science and Art (Grant No.

10-102/414-281-2018). The authors would like to thank the COST Action (CA18135; Fire in the Earth System: Science & Society) for a stimulating working group.

REFERENCES

- Aasly, K., Malvik, T.H., Myrhaug, E., 2007. Advanced methods to characterize thermal properties of quartz. *Infacon*, 11.
- Abraham, J., Dowling, K., Florentine, S., 2017. Risk of post-fire metal mobilization into surface water resources: A review. *Science of the Total Environment*, 599–600, 1740–1755.
- Albalasmeh, A.A., Berli, M., Shafer, D.S., Ghezzehei, T.A., 2013. Degradation of moist soil aggregates by rapid temperature rise under low intensity fire. *Plant and Soil*, 362, 1–2, 335–344. <https://doi.org/10.1007/S11104-012-1408-Z/FIGURES/5>
- Alcañiz, M., Outeiro, L., Francos, M., Úbeda, X., 2018. Effects of prescribed fires on soil properties: A review. *Science of the Total Environment*, 613–614, 944–957.
- Araya, S.N., Meding, M., Berhe, A.A., 2016. Thermal alteration of soil physico-chemical properties: a systematic study to infer response of Sierra Nevada climosequence soils to forest fires. *Soil*, 2, 3, 351–366. <https://doi.org/10.5194/soil-2-351-2016>
- Arcenegui, V., Mataix-Solera, J., Guerrero, C., Zornoza, R., Mayoral, A.M., Morales, J., 2007. Factors controlling the water repellency induced by fire in calcareous Mediterranean forest soils. *European Journal of Soil Science*, 58, 1254–1259.
- Bigham, J.M., Fitzpatrick, R.W., Schulze, D.G., 2002. Iron Oxides. In: Dixon, J.B., Schulze, D.G. (Eds.): *Soil Mineralogy with Environmental Applications*. Soil Science Society of America Book Ser. 7. SSSA, Madison, WI. pp. 323–366.
- Bogunovic, M., Vidacek, Z., Racz, Z., Husnjak, S., Spaka, M., 2011. Soil suitability map for cultivation, Republic of Croatia. In: Panagos, P., Jones, A., Bosco, C., Kumar, P.S. (Eds.): *European digital archive on soil maps (EuDASM): preserving important soil data for public free access*. *International Journal of Digital Earth*, 4, 5, 434–443.
- Boski, T., Herbillon, A.J., 1988. Quantitative determination of hematite and goethite in lateritic bauxites by thermodifferential X-ray powder diffraction. *Clays and Clay Minerals*, 36, 176–180.
- Burke, M.P., Hogue, T.S., Kinoshita, A.M., Barco, J., Wessel, C., Stein, E.D., 2013. Pre- and post-fire pollutant loads in an urban fringe watershed in Southern California. *Environmental Monitoring and Assessment*, 185, 10131–10145.
- Busenberg, E., Clemency, C.V., 1973. Determination of the cation exchange capacity of clays and soils using an ammonia electrode. *Clays and Clay Minerals*, 21, 213–217.
- Campos, I., Abrantes, N., Keizer, J.J., Vale, C., Pereira, P., 2016. Major and trace elements in soils and ashes of eucalypt and pine forest plantations in Portugal following a wildfire. *Science of the Total Environment*, 572, 1363–1376.
- Certini, G., 2005. Effects of fire on properties of forest soils: a review. *Oecologia*, 143, 1–10.
- Commission report, 2020. Europe's nature under threat as world suffers worst year on record for forest fires. https://ec.europa.eu/commission/presscorner/detail/en/ip_20_1995
- Costa, M.R., Calvão A.R., Aranha, J., 2014. Linking wildfire effects on soil and water chemistry of the Marão River watershed, Portugal, and biomass changes detected from Landsat imagery. *Applied Geochemistry*, 44, 93–102.

- Deng, Y., Dixon, J.B., 2002. Soil organic matter and organic-mineral interactions. In: Dixon, J.B., Schulze, D.G. (Eds.): *Soil Mineralogy with Environmental Applications*. Soil Science Society of America Book Ser. 7. SSSA, Madison, WI. pp. 69–107.
- Duane, A., Aquilué, N., Canelles, Q., Morán-Ordoñez, A., de Cáceres, M., Brotons, L. 2019. Adapting prescribed burns to future climate change in Mediterranean landscapes. *Science of the Total Environment*, 677, 68–83. <https://doi.org/10.1016/J.SCITOTENV.2019.04.348>
- Dupuy, J., Fargeon, H., Martin-StPaul, N., Pimont, F., Ruffault, J., Guijarro, M., Hernando, C., Madrigal, J., Fernandes, P., 2020. Climate change impact on future wildfire danger and activity in southern Europe: a review. *Annals of Forest Science*, 77, 2, 1–24. <https://doi.org/10.1007/S13595-020-00933-5>
- EN ISO 10693, 2014. Soil quality - Determination of carbonate content - Volumetric method (ISO [WWW Document], n.d. URL <https://standards.iteh.ai/catalog/standards/cen/822b8ccb-584d-4cd9-8f31-8cdf923f1406/en-iso-10693-2014>
- Fernandez-Marcos, M.L., 2022. Potentially toxic substances and associated risks in soils affected by wildfires: A review. *Toxics*, 10, 1. <https://doi.org/10.3390/TOXICS10010031>
- Francos, M., Úbeda, X., Pereira, P., Alcañiz, M., 2018. Long-term impact of wildfire on soils exposed to different fire severities. A case study in Cadiretes Massif (NE Iberian Peninsula). *Science of the Total Environment*, 615, 664–671.
- García-Corona, R., Benito, E., de Blas, E., Varela, M.E., 2004. Effects of heating on some soil physical properties related to its hydrological behaviour in two north-western Spanish soils. *International Journal of Wildland Fire*, 13, 195–199.
- Gedye, S.J., Jones, R.T., Tinner, W., Ammann, B., Oldfield, F., 2000. The use of mineral magnetism in the reconstruction of fire history: a case study from Lago di Origlio, Swiss Alps. *Palaeogeography, Palaeoclimatology, Palaeoecology*, 164, 101–110.
- Gehring, A.U., Fischer, H., Louvel, M., Kunze, K., Weidler, P.G., 2009. High temperature stability of natural maghemite: a magnetic and spectroscopic study. *Geophysical Journal International*, 179, 3, 1361–1371.
- Gray, D.M., Dighton, J., 2009. Nutrient utilization by pine seedlings and soil microbes in oligotrophic pine barrens forest soils subjected to prescribed fire treatment. *Soil Biology and Biochemistry*, 41, 1957–1965.
- Guo, H., Barnard, A.S., 2013. Naturally occurring iron oxide nanoparticles: morphology, surface chemistry and environmental stability. *Journal of Materials Chemistry A*, 1, 27–42.
- Hajpál, M., Török, Á., 2004. Mineralogical and colour changes of quartz sandstones by heat. *Environ. Geol.*, 46, 311–322.
- Ignatavičius, G., Sakalauskiene, G., Oškinis, V., 2006. Influence of land fires on increase of heavy metal concentrations in river waters of Lithuania. *Journal of Environmental Engineering and Landscape Management*, 14, 1, 46–51, DOI: 10.1080/16486897.2006.9636878
- Inbar, A., Lado, M., Sternberg, M., Tanau, H., Ben-Hur, M., 2014. Forest fire effects on soil chemical and physiochemical properties, infiltration, runoff, and erosion in a semiarid Mediterranean region. *Geoderma*, 221–221, 131–138.
- Ivanić, M., Vdović, N., Barreto, S. de B., Bermanec, V., Sondi, I., 2015. Mineralogy, surface properties and electrokinetic behaviour of kaolin clays from the naturally occurring pegmatite deposits. *Geologia Croatica*, 68, 2, 139–145. <https://doi.org/10.4154/GC.2015.09>
- Kabata-Pendias, A., 2010. *Trace Elements in Soils and Plants*. 4th Edition, 520 p. <https://doi.org/10.1201/B10158/trace-elements-soils-plants-alina-kabata-pendias>
- Kalra, Y.P., 1995. Determination of pH of soils by different methods: collaborative study. *Journal of AOAC International*, 78, 2, 310–324.
- Ketterings, Q.M., Bigham, J.M., Laperche, V., 2000. Changes in soil mineralogy and texture caused by slash-and-burn fires in Sumatra, Indonesia. *Soil Science Society of America Journal*, 64, 1108–1117.
- Li, Y., Zhang, Y., Zhang, Y., Liu, M., Zhang, F., Wang, L., 2017. Thermal behavior analysis of halloysite selected from Inner Mongolia Autonomous Region in China. *Journal of Thermal Analysis and Calorimetry*, 129, 1333–1339.
- Liu, X.M., Shaw, J., Jiang, J.Z., Bloemendal, J., Hesse, P., Rolph, T., Mao, X.G., 2010. Analysis on variety and characteristics of maghemite. *Science China Earth Sciences*, 53, 8, 1153–1162. <https://doi.org/10.1007/S11430-010-0030-2>
- Liu, X., Liu, X., Hu, Y., 2015. Investigation of the thermal behaviour and decomposition kinetics of kaolinite. *Clay Minerals*, 50, 199–209.
- Mammucari, R., 2008. Processing of iron oxide nanoparticles by supercritical fluids. *Industrial and Engineering Chemistry Research*, 47, 599–614.
- Marcos, E., Tárrega, R., Luis, E., 2007. Changes in a Humic Cambisol heated (100–500 °C) under laboratory conditions: The significance of heating time. *Geoderma*, 138, 3–4, 237–243. <https://doi.org/10.1016/J.GEODERMA.2006.11.017>
- Mataix-Solera, J., Zavala, L.M., Jordán, A., Bárcenas-Moreno, G., Lozano, E., Gil-Torres, J., Arcenegui, V., Pérez-Bejarano, A., Morugán-Coronado, A., Jiménez-Pinilla, P., Granged, A.J.P., 2014. Small variations of soil properties control fire-induced water repellency. *Spanish Journal of Soil Science*, 4, 51–60.
- Moore, D.M., Reynolds, R.C.Jr., 1997. *X-Ray diffraction and the identification and analysis of clay minerals*. 2nd Edition, Oxford University Press, New York.
- Moreno, J.M., 2014. *Forest fires under climate, social and economic changes in Europe, the Mediterranean and other fire - affected areas of the world*. FUME. Lessons learned and outlook (Available from: <http://fumeproject.uclm.es>)
- Moriondo, M., Good, P., Durao, R., Bindi, M., Giannakopoulos, C., Corte-Real, J., 2006. Potential impact of climate change on fire risk in the Mediterranean area. *Climate Research*, 31, 85–95.
- Namduri, H., Nasrazadani, S., 2008. Quantitative analysis of iron oxides using Fourier transform infrared spectrophotometry. *Corrosion Science*, 50, 2493–2497.
- Neary, D.G., Ryan, K.C., DeBano, L.F., 2005. *Wildland fire in ecosystems: effects of fire on soils and water*. Gen. Tech. Rep. RMRS-GTR-42-vol.4. Ogden, UT: U.S. Department of Agriculture, Forest Service, Rocky Mountain Research Station, 250 p.
- Nimac, I., Tadić, M.P., 2016. New 1981–2010 climatological normals for Croatia and comparison to previous 1961–1990 and 1971–2000 normals. *Proceedings from GeoMLA conference*, Beograd, pp. 79–85.
- Odigie, K.O., Khanis, E., Hibdon, S.A., Jana, P., Aranea, A., Urrutia, R., Flegla, A.R., 2016. Remobilization of trace elements by forest fire in Patagonia, Chile. *Regional Environmental Change*, 16, 1089–1096.
- Palansooriya, K.N., Shaheen, S.M., Chen, S.S., Tsang, D.C.W., Hashimoto, Y., Hou, D., Bolan, N.S., Rinklebe, J., Ok, Y.S., 2020. Soil amendments for immobilization of potentially toxic elements in contaminated soils: A critical review. *Environment International*, 134, 105046. <https://doi.org/10.1016/J.ENVINT.2019.105046>

- Pape, A., Switzer, C., McCosh, N., Knapp, C. W., 2015. Impacts of thermal and smouldering remediation on plant growth and soil ecology. *Geoderma*, 243–244, 1–9. <https://doi.org/10.1016/J.GEODERMA.2014.12.004>
- Pavlek, K., Bišćević, F., Furčić, P., Grđan, A., Gugić, V., Malešić, N., Moharić, P., Vragović, V., Fuerst-Bjeliš, B., Cvitanović, M., 2016. Spatial patterns and drivers of fire occurrence in a Mediterranean environment: a case study of southern Croatia. *Geografisk Tidsskrift – Danish Journal of Geography*, 117, 22–35.
- Pereira, P., Úbeda, X., 2010. Spatial distribution of heavy metals released from ashes after a wildfire. *Journal of Environmental Engineering and Landscape Management*, 18, 13–22.
- Pereira, P., Cerdà, A., Úbeda, X., Mataix-Solera, J., Rein, G., 2019. *Fire Effects on Soil Properties*. CSIRO Publishing.
- Rauret, G., Lopez-Sanchez, J.F., Sahuquillo, A., Rubio, R., Davidson, C., Ure, A., Quevauviller, P.H., 1999. Improvement of the BCR three step sequential extraction procedure prior to the certification of new sediment and soil reference materials. *Journal of Environmental Monitoring*, 1, 57–61.
- Reynard-Callanan, J.R., Pope, G.A., Gorrington, M.L., Feng, H., 2010. Effects of high-intensity forest fires on soil clay mineralogy. *Physical Geography*, 31, 407–422.
- Ringdalen, E., 2015. Changes in quartz during heating and the possible effects on Si production. *JOM*, 67, 484–492.
- San-Miguel-Ayanz, J., Durrant, T., Boca, R., Maianti, P., Liberta, G., Artes Vivancos, T., Jacome Felix Oom, D., Branco, A., De Rigo, D., Ferrari, D., Pfeiffer, H., Grecchi, R., Nuijten, D., 2022. Advance report on wildfires in Europe, Middle East and North Africa 2021. Publications Office of the European Union, Luxembourg. ISBN 978-92-76-49633-5. DOI:10.2760/039729, JRC128678
- Santín, C., Doerr, S.H., 2016. Fire effects on soils: the human dimension. *Philosophical Transactions of the Royal Society B: Biological Sciences*, 371, 1696. <https://doi.org/10.1098/RSTB.2015.0171>
- Schulze, D.G., 2002. An introduction to soil mineralogy. In: Dixon, J.B., Schulze, D.G. (Eds.): *Soil Mineralogy with Environmental Applications*. Soil Science Society of America Book Ser. 7. SSSA, Madison, WI. pp. 1–35.
- Sennett, P., 1989. Changes in the physical properties of kaolin on exposure to elevated temperature. In: *Proceedings of the 9th international Clay Conference, Strasbourg, 1989. Vol V: Industrial applications of clays. Analytical techniques and teaching of clay mineralogy*. Strasbourg: Institut de Géologie – Université Louis-Pasteur, 1990. pp. 71–79. (*Sciences Géologiques. Mémoire*, 89).
- Sidhu, P.S., 1988. Transformation of trace element-substituted maghemite to hematite. *Clays Clay Miner.* 36, 31–38. <https://doi.org/10.1346/CCMN.1988.0360105>
- Shepard, F.P., 1954. Nomenclature based on sand-silt-clay ratios. *Journal of Sedimentary Research*, 24, 151–158. <https://doi.org/10.1306/D4269774-2B26-11D7-8648000102C1865D>
- Soto, B., Benito, E., Diaz-Fierros, F., 1991. Heat-induced degradation processes in forest soils. *International Journal of Wildland Fire*, 1, 3, 147–152. <https://doi.org/10.1071/WF9910147>
- Soto, B., Diaz-Fierros, F., 1993. Interactions between plant ash leachates and soil. *International Journal of Wildland Fire*, 3, 4, 207–216.
- Šiljković, Ž., Mamut, M., 2016. Forest fires in Dalmatia. *Bulletin of Geography. Socio-Economic Series*, 32, 117–130.
- Tekić, I., Fuerst-Bjeliš, B., Durbešić, A., 2014. Distribution of Aleppo pine (*Pinus halepensis* Mill.) and its effect on vegetation and landscape structure of wider area of Šibenik. *Šumarski list*, 138, 11–12, 593–600. (In Croatian.)
- Thomaz, E.L., Fachin, P.A., 2014. Effects of heating on soil physical properties by using realistic peak temperature gradients. *Geoderma*, 230–231, 243–249. <https://doi.org/10.1016/J.GEODERMA.2014.04.025>
- Úbeda, X., Pereira, P., Outeiro, L., Martin, D.A., 2009. Effects of fire temperature on the physical and chemical characteristics of the ash from two plots of cork oak (*Quercus suber*). *Land Degradation & Development*, 20, 589–608.
- Úbeda, X., Sarricolea, P., 2016. Wildfires in Chile: a review. *Global and Planetary Change*, 146, 152–161.
- Ulery, A.L., Graham, R.C., Bowen, L.H., 1996. Forest fire effects on soil phyllosilicates in California. *Soil Science Society of America Journal*, 60, 309–315.
- Ulery, A.L., Graham, R.C., Goforth, B.R., Hubbert, K.R., 2017. Fire effects on cation exchange capacity of California forest and woodland soils. *Geoderma*, 286, 125–130.
- Vassiliadou, I., Papadopoulou, A., Costopoulou, D., Vasiliadou, S., Christoforou, S., Leondiadis, L., 2009. Dioxin contamination after an accidental fire in the municipal landfill of Tagarades, Thessaloniki, Greece. *Chemosphere*, 74, 879–884.
- Wang, X., Wang, J., Zhang, J., 2012. Comparisons of three methods for organic and inorganic carbon in calcareous soils of northwestern China. *PLoS ONE*, 7, 8, e44334.
- Wentworth, C.K., 1922. A scale of grade and class terms for clastic sediments. *The Journal of Geology*, 30, 377–392.
- Yoon, J., Cao, X., Zhou, Q., Ma, L.Q., 2006. Accumulation of Pb, Cu, and Zn in native plants growing on a contaminated Florida site. *Science of the Total Environment*, 368, 2–3, 456–464. <https://doi.org/10.1016/J.SCITOTENV.2006.01.016>
- Yuan, P., Tan, D., Annabi-Bergaya, F., Yan, W., Fan, M., Liu, D., He, H., 2012. Changes in structure, morphology, porosity, and surface activity of mesoporous halloysite nanotubes under heating. *Clays and Clay Minerals*, 60, 561–573.
- Zobnin, N.N., Torgovets, A.K., Pikalova, I.A., Yussupova, Y.S., Atakishiyev, S.A., 2018. Influence of thermal stability of quartz and the particle size distribution of burden materials on the process of electrothermal smelting of metallurgical silicon. *Oriental Journal of Chemistry*, 34, 2, 1120–1125. <https://doi.org/10.13005/OJC/340265>

Received 7 May 2022

Accepted 9 July 2022

SUPPLEMENTARY INFORMATION

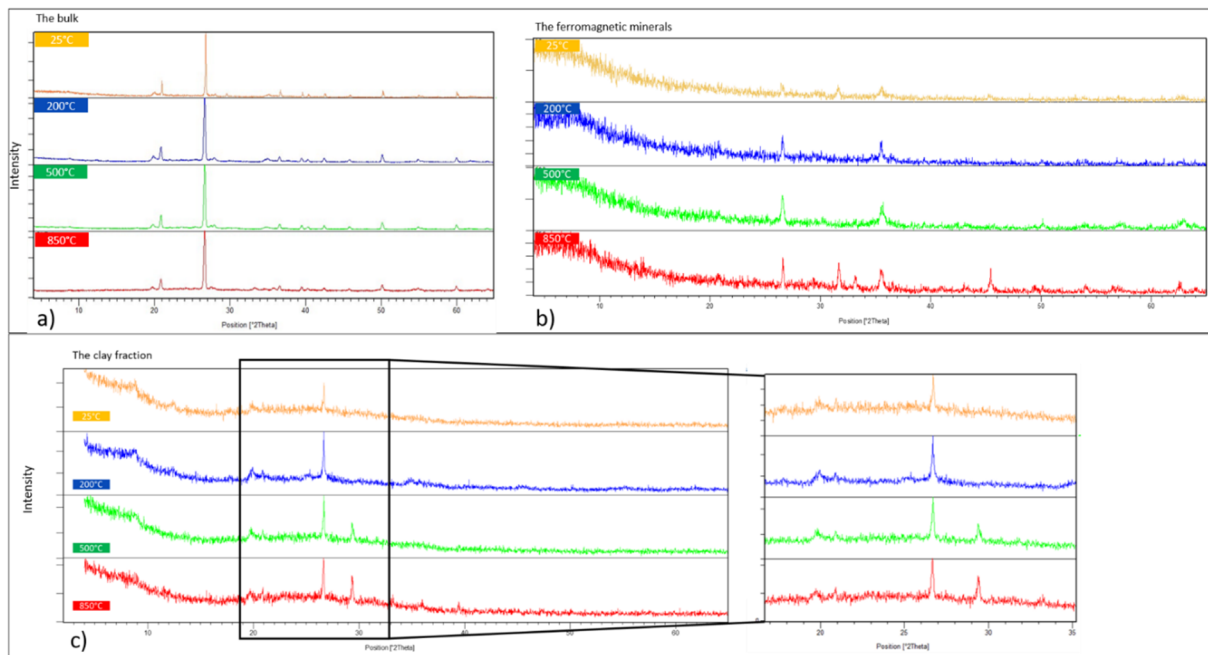


Fig. S1. The XRD analysis of the bulk, ferromagnetic minerals isolated from the bulk and clay fraction.

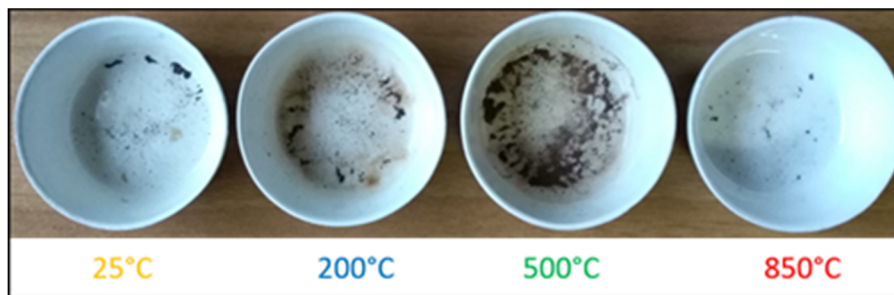


Fig. S2. The ferromagnetic minerals isolated from the bulk samples treated at different temperatures.